Individual-based quantitative temporal beta diversity: Novel indices for assessing community compositional shifts accounting for changes in the properties of individuals

Ryosuke Nakadai

ORCID: 0000-0002-9512-8511

Biodiversity Division, National Institute for Environmental Studies, Onogawa 16-2, Tsukuba, Ibaraki, 305-8506, Japan

E-mail address: r.nakadai66@gmai.com, nakadai.ryosuke@nies.go.jp

Abstract

Revealing the patterns of temporal biodiversity changes due to global climate change and deciphering the connection between individual life histories and large-scale ecological patterns is essential for improving the mechanistic understanding of macroecology; however, this is challenging because the relations between individual life history and biodiversity remain unclear. In the present study, I developed novel indices that allow evaluating community compositional shifts over time by explicitly considering the contributions of the life histories (i.e. growth, mortality, and recruitment) of individuals in a community. The indices were applied to subset data from the US Forest Inventory and Analysis database for the state of Rhode Island (USA) to identify changes in the contribution of individual life histories to biodiversity change. The results of this study not only represent methodological progress in community ecology and macroecology, but also a conceptual advance in bridging studies on biodiversity with those on individual life history and physiology. The individual-based diversity indices pave the way to individual-based biodiversity science, which may facilitate understanding the comprehensive effects of climate change across different hierarchies of biological organisation.

Keywords: climate change, compositional shift, growth, forest dynamics, individual, life-history

1. Introduction

Elucidating patterns of biodiversity change over time has received substantial research attention in light of the effects of global climate change (Dornelas et al., 2014; García et al., 2016; Vellend et al., 2013). Classical studies have focused on biodiversity loss (i.e. alpha and gamma diversity); however, while some studies have attempted to quantify compositional shifts in biodiversity, termed temporal beta diversity (Gotelli et al., 2017; Magurran, 2011), deep knowledge on compositional shifts is lacking (Dornelas et al., 2014; Magurran et al., 2015, 2019). Recent studies have developed unique methodologies and concepts for measuring temporal beta diversity based on classical spatial beta-diversity research (Gotelli et al., 2021; Legendre, 2019; Shimadzu, et al., 2015; Tatsumi et al., 2021).

An individual cannot exist in two places simultaneously, but it can persist in the same habitat over time (Magurran et al., 2019). Therefore, individual persistence and turnover are important factors for measuring temporal beta diversity. In fact, individuals of long-lived species (e.g. trees and vertebrates) can persist over the long term, whereas individuals of short-lived species are replaced by conspecifics or individuals of other species (Nakadai, 2020, 2021). Nakadai (2020) proposed the concept of 'individual-based beta diversity' to bridge the gap between biodiversity and individual information and provided novel indices to evaluate individual turnover and compositional shifts based on comparisons between two periods at a given site. Specifically, Nakadai (2020) developed an individual-based temporal beta-diversity approach for the Bray–Curtis dissimilarity index (i.e. an abundance-based temporal beta-diversity index). In other words, Nakadai (2020, 2021) added both persistence and turnover of individuals to the compositional shifts in biodiversity over time.

Climate change is known to directly affect not only biodiversity, but also the individual life histories of organisms (Brienen et al., 2020; Searle & Chen, 2018). Recent studies have shown that climate warming will accelerate the growth and shorten the life spans—which are determined by physiological processes—of individual trees (Körner, 2017; Munné-Bosch, 2018; Searle & Chen, 2018) and increase the amount of carbon stocks in terrestrial ecosystems (Brienen et al., 2015). Such changes in individual life histories potentially affect the compositional shifts of local communities and consequently, global biodiversity. While

understanding the connection between individual physiology and large-scale ecological patterns is essential for a mechanistic understanding of macroecology (Brown, 1995, 1999; Brown et al. 2004; e.g. metabolic theory), it is challenging because the connection between individual life history and biodiversity remains unknown. To comprehensively understand the effects of climate change, it is essential to simultaneously capture property changes in individuals, individual turnover, and compositional shifts in biodiversity.

Despite these needs, previous approaches to individual-based temporal beta diversity (Nakadai, 2020, 2021) only considered the presence or absence of each individual (e.g. qualitative properties such as 'dead' or 'alive'), and the influences on biodiversity of property changes in each individual (e.g. individual growth) over time on biodiversity have been neglected. Therefore, the purpose of this study was to develop new individual-based temporal beta-diversity indices that can assess compositional shifts over time by explicitly including property changes in each individual in a community. Hereafter, I call the indices developed in Nakadai (2020) and the novel indices introduced in the present study individual-based 'qualitative' ('QL') indices and individual-based 'quantitative' ('QT') indices, respectively. By introducing quantitative individual information (e.g. size and weight), these novel indices can evaluate the contribution of individual growth and the differences between large and small individuals. After briefly reviewing the history of pairwise beta-diversity indices, I extend individual-based QL temporal beta-diversity indices to QT indices. I then apply these indices to subset data from the US Forest Inventory and Analysis (FIA) database for the state of Rhode Island in the USA (Stanke et al., 2020, Burrill et al., 2021) as a case study to demonstrate their application.

2. Materials and methods

2.1. Conventional incidence-based and abundance-based indices and recently developed individual-based qualitative (QL) temporal beta-diversity indices

Incidence-based and abundance-based beta-diversity indices have been previously proposed (Baselga, 2013). For example, the widely used Bray–Curtis dissimilarity index (Odum, 1950) is an abundance-based extension of the Sørensen index (Baselga, 2013; Legendre &

Legendre, 2012; Sørensen, 1948). Incidence-based methods target the number of species, whereas abundance-based methods mainly target the number of individuals and sometimes, area, biomass, weight, etc. (e.g. Li et al., 2016). I describe this approach in more detail in the present paper. Conventional beta-diversity indices are based on intersection (A, a) and relative complement (B, b, C, c) components. Hereafter, I explain only the context of temporal beta-diversity. Specifically, the Sørensen dissimilarity index (d_{sor}; Sørensen, 1948) is formulated as follows:

$$d_{sor} = \frac{b+c}{2a+b+c} \qquad \text{Eqn. 1}$$

where a is the number of species common to both temporal units; b is the number of species that occur in the first, but not the second temporal unit; and c is the number of species that occur in the second, but not the first temporal unit. Analogously, the Bray–Curtis dissimilarity index (d_{BC}; Odum, 1950) is formulated as follows:

$$d_{BC} = \frac{B+C}{2A+B+C} \qquad \text{Eqn. 2}$$

As a premise for explanation, assume that there are two sets of community data along the time axis—communities at time j and time k (abbreviated as Tj and Tk: $j < k$), respectively. The abundance-based components are as follows:

$$A = \sum_i \min(x_{ij}, x_{ik}) \qquad \text{Eqn. 3q}$$

$$B = \sum_i \left[x_{ij} - \min(x_{ij}, x_{ik})\right] \qquad \text{Eqn. 3b}$$

$$C = \sum_i \left[x_{ik} - \min(x_{ij}, x_{ik})\right] \qquad \text{Eqn. 3c}$$

where x_{ij} is the abundance of species i at temporal unit j, and x_{ik} is the abundance of species i at temporal unit k. Therefore, A is the number of individuals of each species shared by units j and k, and B and C are the numbers of individuals unique to units j and k, respectively.

Nakadai (2020) introduced the categorisation of the community dynamics component into

persistence (p), mortality (m), and recruitment (r) in individual-based temporal beta-diversity. m refers to the number of individuals occurring at Tj that die before Tk, representing the total number of individuals that died during the time between Tj and Tk. r identifies the number of individuals that were not yet alive at Tj (or were not yet in the size class counted), but were alive and counted at Tk, representing the total number of individuals recruited between Tj and Tk. Component p refers to the persistence of individuals from Tj to Tk. Note that, unlike previous studies (Nakadai, 2020, 2021; Fig. 1a), I use lower-case letters for the components of individual-based qualitative indices (i.e. p, m, r) to distinguish the components of the individual quantitative indices described later. Thus, the abundances are calculated as follows:

$$p = \sum_o \min(z_{oj}, z_{ok}) \quad \text{Eqn. 4a}$$

$$m = \sum_o \left[z_{oj} - \min(z_{oj}, z_{ok})\right] \quad \text{Eqn. 4b}$$

$$r = \sum_o \left[z_{ok} - \min(z_{oj}, z_{ok})\right] \quad \text{Eqn. 4c}$$

where z_{oj} is individual o at time Tj, and z_{ok} is individual o at time Tk. Both z_{oj} and z_{ok} have values of one or zero (presence and absence, respectively). Therefore, p is the total number of individuals present at both Tj and Tk, and m and r are the numbers of individuals unique to Tj and Tk, respectively (Nakadai, 2020, 2021; Fig. 1a).

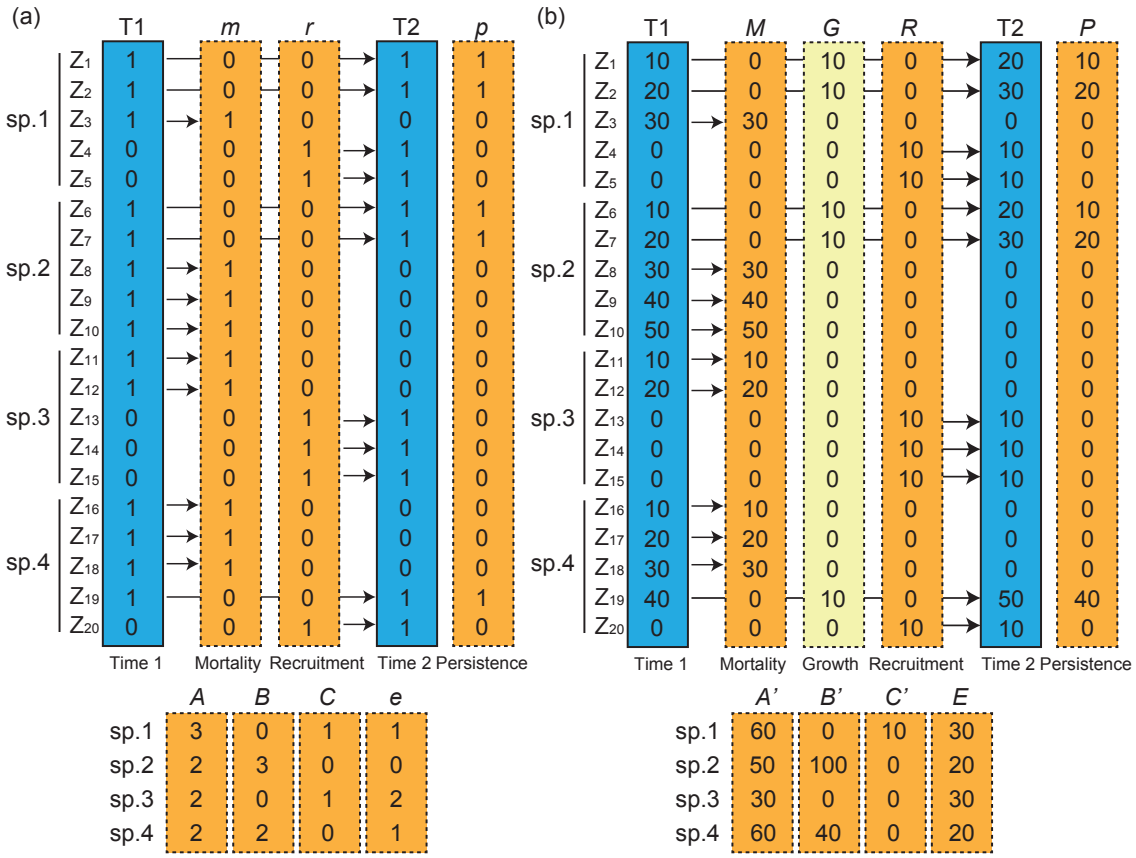

Fig. 1. Schematic representation of individual-based temporal beta diversity for both qualitative (a) and quantitative (b) components. T1 and T2 refer to the communities at times 1 and 2, respectively. Both communities T1 and T2 comprise four species (sp. 1, 2, 3, and 4), and all individuals are identified separately (Z_o) in both cases. The arrows indicate the temporal trajectory for each individual. In the qualitative component (a), *m* refers to the number of individuals in existence at T1, but dead before T2, thereby separately identifying the deaths of individuals during the period between T1 and T2; *r* identifies the number of individuals that were not yet alive at T1, but were at T2, thereby identifying the recruitment of individuals during the period between T1 and T2; *p* refers to individuals that persisted from T1 to T2, thus both T1 and T2 = 1. In the qualitative component (b), *M* refers to the total measures of individuals occurring at T1 that die before T2, thereby representing the total measures of the mortal individuals during the time between T1 and T2; *R* identifies the total measures of individuals that were not yet alive at T1, but were alive and counted at T2, thereby representing the individuals recruited between T1 and T2. Persistent individuals are qualitatively identical, having alive (or present) status between T1 and T2, but rarely maintain the same status with respect to size and weight. Therefore, changes in individual properties occur between T1 and T2. The quantitative indices consider

the contribution of changes in individuals' properties, mainly targeting individual growth. Specifically, for persistent individuals, the original and altered total measures are partitioned into persistent (*P*) and growth (*G*) components, respectively.

The individual-based temporal beta-diversity index for Bray–Curtis dissimilarity (d_{mr}) can be formulated as follows:

$$d_{mr} = \frac{m+r}{2p+m+r} \qquad \text{Eqn. 5}$$

In some cases, there is a turnover of different individuals belonging to the same species, even when the community composition is stable over time. Therefore, the components that change over time (*m* and *r*) are reorganised into two further components, namely compositional equilibrium (*e*) and shift (*B* and *C*) (Nakadai, 2020, 2021). Component *m* can be partitioned into two additive components: the lost individuals that contribute to compositional shifts in a community (*B*) and lost individuals replaced by conspecifics that contribute to an equilibrium in community composition (e_{loss}) (Fig. 1a). Similarly, component *r* can be partitioned into two additive components: gained individuals that contribute to compositional shifts in a community (*C*) and gained individuals that replace conspecifics, thereby contributing to an equilibrium in community composition (e_{gain}) (Fig. 1a). By definition, the numbers of e_{loss} and e_{gain} individuals are identical; thus, I replaced both e_{loss} and e_{gain} with the coefficient *e* (Nakadai, 2020, 2021). The persistence component (*p*) is the shared (apparent non-changed) component (*A*) minus the equilibrium (changed, but apparent non-changed) component (*e*) of community composition. The above descriptions are summarized below:

$$e_{loss} = e_{gain} = e \qquad \text{Eqn. 6}$$

$$m = B + e \qquad \text{Eqn. 7}$$

$$r = C + e \qquad \text{Eqn. 8}$$

$$p = A - e \qquad \text{Eqn. 9}$$

Furthermore, components *m* and *r* can be analysed in the same manner as the community data (Nakadai, 2020). Therefore, the Bray–Curtis dissimilarity between communities can be calculated based on *m* and *r* (Fig. S1d) as follows:

$$v_{s.QL} = \frac{B+C}{2e+B+C} = \frac{B+C}{m+r} \qquad \text{Eqn. 10}$$

where $v_{s.QL}$ indicates the speed of compositional shifts in a community relative to the total speed of individual turnover associated with *m* and *r*. In other words, $v_{s.QL}$ indicates total changes in community composition divided by total changes in the number of individuals. It is possible to calculate $v_{s.QL}$ as d_{BC} divided by d_{mr} as:

$$d_{BC} \div d_{mr} = \frac{B+C}{2A+B+C} \div \frac{m+r}{2p+m+r} = \frac{B+C}{2(p+e)+B+C} \div \frac{m+r}{2p+m+r} = \frac{B+C}{2o+m+r} \div \frac{m+r}{2p+m+r} = \frac{B+C}{2e+B+C} = v_{s.QL} \qquad \text{Eqn. 11}$$

2.2. Novel individual-based "quantitative (QT)" beta-diversity indices

I developed individual-based QT components and novel indices for community datasets over time using individual property information (e.g. size and weight). The relationship between the QL and QT indices is similar to that between the incident-based and abundance-based indices. In other words, individual-based QT components were calculated as individual-based QL weighted by individual properties. As previously noted, the abundance targeted by abundance-based indicators is not necessarily the number of individuals, but can also include area, volume, etc. Abundance measures excluding the number of individuals for community datasets have been used in cases of large size variation among individuals within a community or where it is difficult to recognise proper individuals (Li et al., 2016). Hereafter, the Bray–Curtis indices targeting measures excluding the number of individuals (e.g. sizes and weights) are described as $d_{BC'}$, and their components are described with apostrophes (*A'*, *B'*, and *C'*) to distinguish them from the components in the unweighted Bray–Curtis index as follows:

$$d_{BC'} = \frac{B'+C'}{2A'+B'+C'} \qquad \text{Eqn. 12}$$

This weighting indicates that abundance-based (number of individual-based) diversity indices were weighted by total measures of individuals for each species, thus calculating diversity indices by implicitly considering the variation in measures of each individual. Because individuality is rarely clearly identifiable in weighted indices, this relationship is not well recognised.

In addition to individual-based QL indices, individual-based QT indices comprise components of mortality and recruitment (*M* and *R*, respectively). In the QT indices, *M* refers to the total number of measures of individuals occurring at T*j* that die before T*k*, representing the total number of measures of the individuals that died between T*j* and T*k* (Fig. 1b). *R* identifies the total number of measures of individuals that were not yet alive at T*j* (or were not yet in the size class counted), but were alive and counted at T*k*, representing the total number of measures of the individuals recruited between T*j* and T*k* (Fig. 1b).

From this point on, the major differences between the QL and QT indices are as follows. The persistent individuals are qualitatively identical, maintaining their alive (or present) status between T*j* and T*k*, but rarely maintain the same status in terms of size and weight; thus, there is a change in individual properties between T*j* and T*k*. For example, in tree communities, one newly recruited small tree can be a large tree after persisting for half a century. In the *p* component of QL indices, this means that an individual is persistent, while it is impossible to evaluate changes in its features (e.g. basal area, biomass, and/or weight). The indices introduced here overcome this problem by considering the contribution of changes in individual properties, mainly targeting individual growth. Specifically, in the case of persistent individuals, the original and altered total number of measures are partitioned into persistent (*P*) and growth (*G*) components, respectively. Thus, the respective total number of measures of the components are calculated as follows:

$$M = \sum_o \left[\left[w_{oj} - \min\left(w_{oj}, w_{ok}\right)\right] \times \left[z_{oj} - \min\left(z_{oj}, z_{ok}\right)\right]\right] \qquad \text{Eqn. 13a}$$

$$R = \sum_o \left[\left[w_{ok} - \min\left(w_{oj}, w_{ok}\right)\right] \times \left[z_{ok} - \min\left(z_{oj}, z_{ok}\right)\right]\right] \qquad \text{Eqn. 13b}$$

$$P = \sum_o \min(w_{oj}, w_{ok}) \qquad \text{Eqn. 13c}$$

$$G = \sum_o \left[\left[\max(w_{oj}, w_{ok}) - \min(w_{oj}, w_{ok})\right] \times \min(z_{oj}, z_{ok})\right] \qquad \text{Eqn. 13d,}$$

where w_{oj} is the measure of individual o at time Tj, and w_{ok} is the measure of individual o at time Tk. M and R are the total number of measures of demised and recruited individuals, respectively. The persistent and growth components represent the unchanged and changed components of measures within an individual between Tj and Tk, respectively. Thus, P and G represent the total amount of these components within a community. Equation 13d also considers decreases in the measures of each individual. Therefore, the calculation of the G component can be partitioned into increasing and decreasing components, as follows:

$$G = \sum_o \left[\left[\max(w_{oj}, w_{ok}) - \min(w_{oj}, w_{ok})\right] \times \min(z_{oj}, z_{ok})\right] = G_{in} + G_{de} \qquad \text{Eqn. 14,}$$

where G_{in} and G_{de} are the total increased and decreased components of the targeted measures, respectively. Specifically, the formulas for G_{in} and G_{de} are as follows:

$$G_{in} = \sum_o \left[\left[w_{ok} - \min(w_{oj}, w_{ok})\right] \times \min(z_{oj}, z_{ok}) \times \frac{1}{2}\left[1 + \text{sign}(w_{ok} - w_{oj})\right]\right] \qquad \text{Eqn. 15a}$$

$$G_{de} = \sum_o \left[\left[w_{oj} - \min(w_{oj}, w_{ok})\right] \times \min(z_{oj}, z_{ok}) \times \frac{1}{2}\left[1 - \text{sign}(w_{ok} - w_{oj})\right]\right] \qquad \text{Eqn. 15b,}$$

where $\frac{1}{2}\left[1 + \text{sign}(w_{ok} - w_{oj})\right]$ and $\frac{1}{2}\left[1 - \text{sign}(w_{ok} - w_{oj})\right]$ distinguish the large and small relationships between w_{ok} and w_{oj} by returning 1 or 0.

This formulation of the individual-based QT temporal beta-diversity index for Bray–Curtis dissimilarity (d_{MRG}) can be expressed as follows:

$$d_{MRG} = \frac{M+R+G}{2P+M+R+G} \qquad \text{Eqn. 16}$$

Further, this individual-based QT temporal beta diversity can be partitioned into the relative contributions of mortality (d_M), recruitment (d_R), and growth (d_G) to the target weights or measurements, as follows:

$$d_{MRG} = \frac{M+R+G}{2P+M+R+G}$$
$$= \frac{M}{2P+M+R+G} + \frac{R}{2P+M+R+G} + \frac{G}{2P+M+R+G} = d_M + d_R + d_G \qquad \text{Eqn. 17}$$

In addition, as shown in equations 15a and b, the G component can be partitioned into G_{de} and G_{in}, which are the total decrease and increase, respectively, in the targeted measures. Equation 17 can then be partitioned into two components, as follows:

$$d_{MRG} = \frac{M+R+G}{2P+M+R+G}$$
$$= \frac{M+G_{de}}{2P+M+R+G} + \frac{R+G_{in}}{2P+M+R+G} = d_{de} + d_{in} \qquad \text{Eqn. 18}$$

where d_{de} and d_{in} indicate the contributions of the decrease and increase, respectively, to the total changes in the targeted measures in T*j* and T*k*. In addition to the QL indices (Nakadai, 2020, 2021), the components that change over time (*M*, *R*, and *G*) can be reorganised into two additive components: compositional equilibrium (*E*) and shift (*B'* and *C'*). Component $M + G_{de}$ can be reorganised as the total number of lost measures that contribute to compositional shifts in a community (*B'*) and the total number of lost measures replaced by conspecifics, contributing to the equilibrium in community composition (E_{loss}) (Fig. 1b). Similarly, component $R + G_{in}$ can be reorganised as the total number of measures that contribute to compositional shifts in a community (*C'*) and the total number of gained measures replacing conspecifics, contributing to the equilibrium in community composition (E_{gain}) (Fig. 1b). By definition, the total amounts of E_{loss} and E_{gain} are identical; hence, I replaced both E_{loss} and E_{gain} with coefficient *E*. In addition, the persistence component (*P*) is the shared (apparent non-changed) component (*A'*) minus the community composition equilibrium (changed, but apparent non-changed) component (*E*). The above descriptions can be summarized as follows:

$$E_{loss} = E_{gain} = E \qquad \text{Eqn. 19}$$

$$M + G_{de} = B + E \qquad \text{Eqn. 20}$$

$$R + G_{in} = C + E \qquad \text{Eqn. 21}$$

$$P = A' - E \qquad \text{Eqn. 22}$$

The formulation of the individual-based QT beta-diversity index for Bray–Curtis (d_{MRG}) dissimilarity can be partitioned into two components, contribution to compositional shifts (d_S) and equilibrium (d_E), as follows:

$$d_{MRG} = \frac{M+R+G}{2P+M+R+G} = \frac{M+G_{de}}{2P+M+R+G} + \frac{R+G_{in}}{2P+M+R+G}$$
$$= \frac{E+B}{2P+M+R+G} + \frac{E+C}{2P+M+R+G} = \frac{2E}{2P+M+R+G} + \frac{B+C}{2P+M+R+G} = d_S + d_E \qquad \text{Eqn. 23}$$

Furthermore, components M, R, and G (i.e. $M + G_{de}$ and $R + G_{in}$) can be analysed in the same manner as the community data. Therefore, the Bray–Curtis dissimilarity between communities (i.e. the total amount of lost and gained measures) can be calculated based on M, R, and G (Fig. S1h), as follows:

$$v_{s.QT} = \frac{B'+C'}{2E+B'+C'} = \frac{B'+C'}{M+R+G} \qquad \text{Eqn. 24}$$

where $v_{s.QT}$ indicates the relative speed of compositional shifts in a community against the total turnover of targeted measures associated with M, R, and G. In other words, $v_{s.QT}$ indicates total changes in community composition divided by total changes in targeted measures. If $v_{s.QT}$ is 0, the turnover of the targeted measures does not contribute to compositional shifts in a community, whereas if $v_{s.QT}$ is 1, all turnover of the targeted measures does contribute to the compositional shifts. $v_{s.QT}$ can be calculated as $d_{BC'}$ divided by d_{MRG}, as follows:

$$d_{BC'} \div d_{MRG} = \frac{B'+C'}{2A'+B'+C'} \div \frac{M+R+G}{2P+M+R+G} = \frac{B'+C'}{2(P+E)+B'+C'} \div \frac{M+R+G}{2P+M+R+G} = \frac{B'+C'}{2P+M+R+G} \div \frac{M+R+G}{2P+M+R+G} = \frac{B'+C'}{M+R+G} = v_{s.QT} \qquad \text{Eqn. 25}$$

Here, I focus only on an extension of Bray–Curtis dissimilarity. In Supplementary Text 1, I summarise individual-based beta diversity using the Ružička dissimilarity index (Ružička, 1958), which was identified by Podani et al. (2013) and Legendre (2014) as an appropriate index for beta-diversity studies. The Ružička dissimilarity index is an abundance-based extension of the Jaccard dissimilarity index (Jaccard, 1901).

2.3. Hypothetical impacts of climate warming on compositional shifts in forest communities

The hypothetical impacts of climate warming on compositional shifts, especially in forest communities, are summarized in schematic diagrams for three simple scenarios of forest compositional dynamics ((a) no climate warming, (b) compositional dynamic changes due to warming, and (c) accelerated growth and shortened life span due to warming) in Fig. 2. In scenario (b), it is assumed that the species composition of recruit individuals (i.e., changes of species pool) become different from species in a community during the previous time step. Hence, the proportions of compositional shift (B and C in $v_{s.QL}$ and B' and C' in $v_{s.QT}$ increase) increase during transitional periods. However, the total growth of individuals that have persist since before climate warming acts as a factor decreasing the apparent compositional shift in size-weighted indices (E in $v_{s.QT}$ increase). Scenarios (b) and (c) are represented separately for easy understanding, but they can simultaneously occur and facilitate compositional shifts in forests. In scenario (c), it is assumed that the speed of growth is twice that in scenarios (a) and (b); therefore, life spans become shorter and thus, the turnover of both individuals and target measures increases. In contrast to scenario (b), I did not assume a change in the species pool in scenario (C) and thus, the values of both $v_{s.QL}$ and $v_{s.QT}$ do not change, but rather, the total amount of turnover (d_{mr} and d_{MRG}) increases. Mathematically, if $v_{s.QL}$ and $v_{s.QT}$ are constant, total amount of turnover (d_{mr} and d_{MRG}) is directly linked to the apparent compositional shift (d_{BC} and $d_{BC'}$). Individual growth largely contributes to the fluctuation in compositional shift under accelerated growth as it is more variable than individual turnover, even if the life spans become shorter. Although individuals that died due to causes other than having reached the natural life span (random death and death by

environmental filtering in nature) were not considered because of the complexity of visualization in Fig. 2, in scenarios (b) and (c), such deaths may facilitate compositional shifts, specifically via increasing $v_{s.QL}$ and $v_{s.QT}$ or d_{mr} and d_{MRG}.

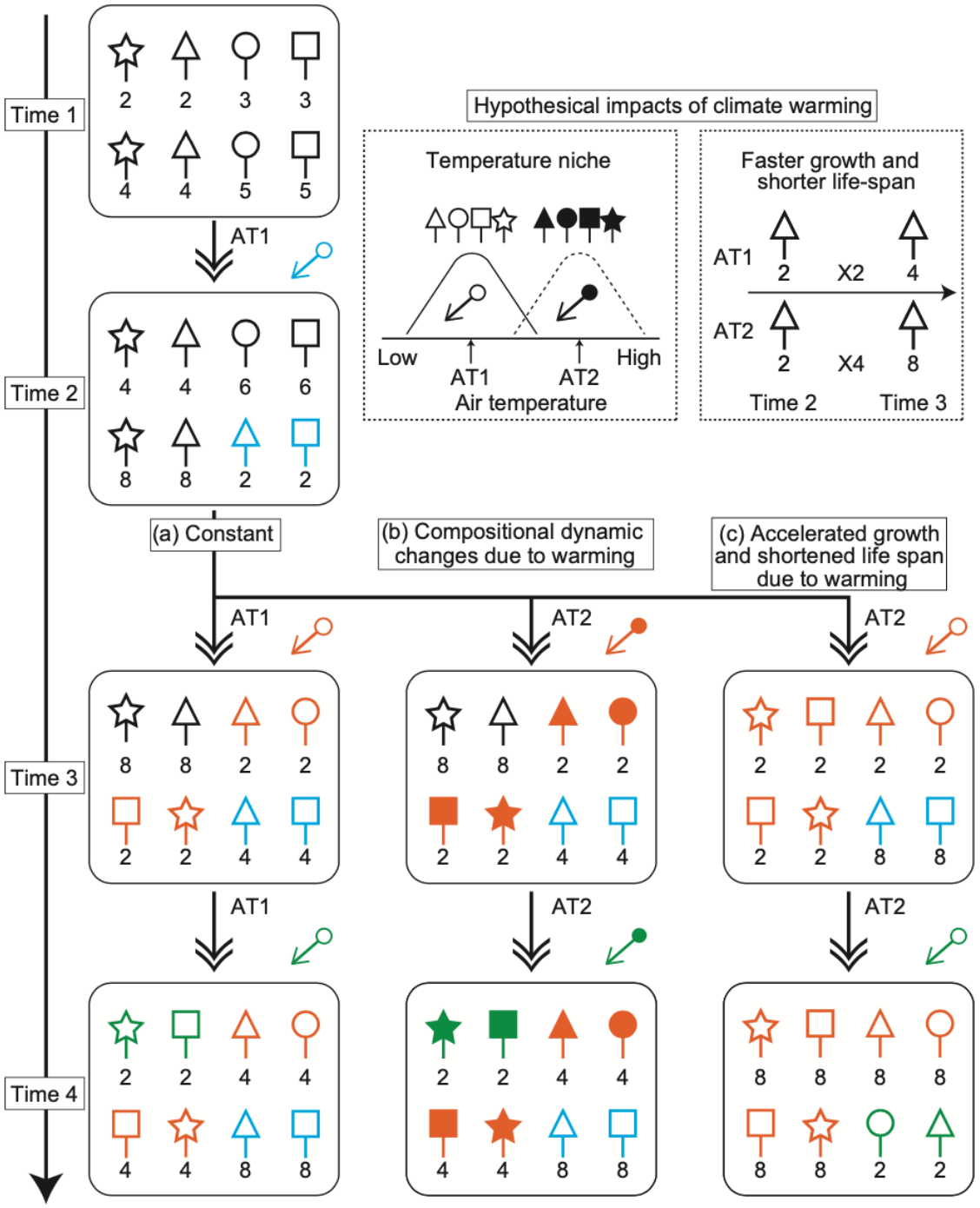

Fig. 2. Schematic diagrams of hypothetical impacts of climate warming on compositional shifts in forest communities. In the figure, three scenarios are shown: (a) no climate warming ('Constant', used as a comparator for the following two scenarios), (b) compositional dynamic changes due to warming, and (c) accelerated growth and shortened life span due to warming. Scenarios (b) and (c) separately show two types of potential

impacts of climate warming on forest dynamics. Different symbols (in terms of filled/unfilled as well as shape) represent individuals of different species (i.e. eight tree species are represented in this figure). The numbers under the symbols indicate individual size, and for simplicity, it is assumed that individuals reaching 10 die. If an individual dies, an individual (size 2) is randomly recruited from the species pool. Two types of species pools were considered along air temperature differences (i.e. AT1 and AT2). Basically, it is assumed that for every one-time step forward, the number doubles (e.g. from 2 to 4). The symbols of individuals in starting communities are coloured black. Symbols in colours other than black indicate individuals recruited at time 2 (blue), time 3 (red), or time 4 (green). The coloured arrows with a circle (top right in each time step) indicate the type of species pool (filled or unfilled symbols). 'AT1' and 'AT2' indicate the temperature condition, i.e. no warming (i.e. constant temperature) or warming (i.e. increase in temperature). The period between time 1 and time 2 is shared among the three scenarios, and differences occur only after this period. In scenario (a) 'constant', it is assumed that the air temperature is constant (i.e. AT1) throughout all time periods; thus, all individuals are recruited from species indicated with unfilled symbols. Scenario (a) is included for comparison between conventional and warming conditions. In both scenarios (b) and (c), it is assumed that the temperature increases from AT1 to AT2 after time 2. In scenario (b) 'compositional dynamic changes', the species pools of recruited individuals shift from unfilled-symbol species to filled-symbol species. After time 2, all recruited individuals are filled-symbol species under scenario (b); thus, until the composition completely shifts from unfilled-symbol species to filled-symbol species, the contribution of individual turnover to compositional equilibrium becomes smaller than that in the conventional condition (scenario (a)). In scenario (c) 'accelerated growth and shortened life span', the speed of growth increases (e.g. from 2 to 4), life spans become shorter, and turnover of both individuals and target measures increase as a result. Note that for simplicity of the visualization, deaths other than those due to having reached natural life spans are not considered.

2.4. Case study using subset data from the FIA database for the state of Rhode Island (USA)

For a case study application of the new individual-based QT indices based on publicly available data, I used a subset of data from the United States Department of Agriculture Forest Service's FIA Program for the state of Rhode Island and the R package rFIA (Stanke et al., 2020). The FIA database includes individual tree-tracking and size information (i.e. basal area and bole biomass). A comprehensive summary of the included data and sampling methodology is provided by Burrill et al. (2021). Briefly, each FIA plot comprises four 0.017-ha circular subplots, each located within a circular 0.10-ha macroplot. All free-

standing woody stems (alive and dead) with a diameter at breast height (DBH) of ≥12.7 cm were sampled within each subplot (Burrill et al., 2021).

The original dataset includes 10,093 individual time records for 58 species, including multiple species (spp.) in 140 plots, from 2004 to 2018. For some plots, there were more than two surveys; therefore, it was possible to calculate more than one value of temporal beta diversity. I conducted plot-level filtering of the datasets using the following criteria: (1) datasets with unidentified individuals at the species level were excluded; (2) datasets with 10 individuals or more were included; and (3) an interval of 5 ± 1 years between two surveys was targeted. In addition, individual trees with a DBH of ≥12.7 cm were targeted because bole biomass was also estimated. The final dataset included 5,705 individual time records comprising 2,541 individual trees of 32 species across 126 survey intervals (86 unique plots). The latitudinal and longitudinal ranges in the dataset are 41.39446°–42.00797° N and 71.79635°–71.12814° W, respectively. The elevation range was 10–680 m. The geographical location of each plot is shown in Fig. S2.

I focused on the basal area and bole biomass of each tree as changes in individual properties that can be considered in the novel indices developed in the previous sections. The basal area of live trees was calculated as $\frac{DBH}{2} \times \frac{DBH}{2} \times \pi$. The gross cubic-foot volume of live trees was estimated at ≥12.7-cm DBH, defining the total volume of wood in the central stem of the inventoried trees (bole biomass) assuming a 30.48-cm mean stump height and a minimum 10.16-cm top diameter (for a detailed estimation method, see Domke et al., 2013).

439 Table 1. Summary of indices and formulae developed in previous studies and used in this study.

Index	Formula	Reference	Ecological interpretation
d_{BC}	$\frac{B+C}{2A+B+C} = \frac{\sum_i [x_{ij} - \min(x_{ij}, x_{ik})] + \sum_i [x_{ik} - \min(x_{ij}, x_{ik})]}{2[\sum_i \min(x_{ij}, x_{ik})] + \sum_i [x_{ij} - \min(x_{ij}, x_{ik})] + \sum_i [x_{ik} - \min(x_{ij}, x_{ik})]}$	Odum (1950)	The compositional shift based on the change in the number of individuals for each species in a community across two time periods ($0 \leq d_{BC} \leq 1$).
d_{mr}	$\frac{m+r}{2p+m+r} = \frac{\sum_o [z_{oj} - \min(z_{oj}, z_{ok})] + \sum_o [z_{ok} - \min(z_{oj}, z_{ok})]}{2[\sum_o \min(z_{oj}, z_{ok})] + \sum_o [z_{oj} - \min(z_{oj}, z_{ok})] + \sum_o [z_{ok} - \min(z_{oj}, z_{ok})]}$	Nakadai (2020)	The individual

			turnover by mortality and recruitment in a community across two time periods ($0 \leq d_{mr} \leq 1$).
$v_{s.QL}$	$\frac{B+C}{2e+B+C} = \frac{B+C}{m+r} = \frac{\sum_i [x_{ij} - \min(x_{ij}, x_{ik})] + \sum_i [x_{ik} - \min(x_{ij}, x_{ik})]}{2[\sum_i \min(x_{ij}, x_{ik}) - \sum_o \min(z_{oj}, z_{ok})] + \sum_i [x_{ij} - \min(x_{ij}, x_{ik})] + \sum_i [x_{ik} - \min(x_{ij}, x_{ik})]}$	Nakadai (2020)	The relative speed of compositional shift in relation to individual turnover ($0 \leq v_{s.QL} \leq 1$).

$d_{BC'}$	$\frac{B'+C'}{2A'+B'+C'} = \frac{\sum_i [y_{ij} - \min(y_{ij}, y_{ik})] + \sum_i [y_{ik} - \min(y_{ij}, y_{ik})]}{2[\sum_i \min(y_{ij}, y_{ik})] + \sum_i [y_{ij} - \min(y_{ij}, y_{ik})] + \sum_i [y_{ik} - \min(y_{ij}, y_{ik})]}$	Odum (1950)	The compositional shift based on the changes in the targeted measures in a community across two time periods ($0 \leq d_{BC'} \leq 1$).
d_{MRG}	$\frac{M+R+G}{2P+M+R+G} = \frac{\sum_o [[w_{oj} - \min(w_{oj}, w_{ok})] \times [z_{oj} - \min(z_{oj}, z_{ok})]] + \sum_o [[w_{ok} - \min(w_{oj}, w_{ok})] \times [z_{ok} - \min(z_{oj}, z_{ok})]] + \sum_o [[\max(w_{oj}, w_{ok}) - \min(w_{oj}, w_{ok})] \times \min(z_{oj}, z_{ok})]}{2[\sum_o \min(w_{oj}, w_{ok}) + \sum_o [[w_{oj} - \min(w_{oj}, w_{ok})] \times [z_{oj} - \min(z_{oj}, z_{ok})]] + \sum_o [[w_{ok} - \min(w_{oj}, w_{ok})] \times [z_{ok} - \min(z_{oj}, z_{ok})]] + \sum_o [[\max(w_{oj}, w_{ok}) - \min(w_{oj}, w_{ok})] \times \min(z_{oj}, z_{o}$	This study	The turnover of the targeted measures by growth, mortality,

			and recruitment in a community across two time periods ($0 \leq d_{MRG} \leq 1$).
$v_{s.QT}$	$\frac{B' + C'}{2E + B' + C'} = \frac{\sum_i [y_{ij} - \min(y_{ij}, y_{ik})] + \sum_i [y_{ik} - \min(y_{ij}, y_{ik})]}{2[\sum_i \min(y_{ij}, y_{ik}) - \sum_o \min(w_{oj}, w_{ok})] + \sum_i [y_{ij} - \min(y_{ij}, y_{ik})] + \sum_i [y_{ik} - \min(y_{ij}, y_{ik})]}$	This study	The relative speed of compositional shift in relation to the turnover of the target measure ($0 \leq v_{s.QT} \leq 1$).

x_{ij} is the abundance of species i at temporal unit j, and x_{ik} is the abundance of species i at temporal unit k. y_{ij} is abundance excluding individuals (i.e. measures or weights) of species i at time Tj at a site, and y_{ik} is abundance excluding individuals of species i at time Tk at a site. w_{oj} is the measure of individual o at time Tj, and w_{ok} is the measure of individual o at time Tk. The equations of d_{BC} and $d_{BC'}$ are mathematically same and the difference is only in the target abundances.

To demonstrate the application of the novel indices, I focused mainly on the following 11 indices: d_{BC}, d_{mr}, d_m, d_r, $v_{s.QL}$, $d_{BC'}$, d_{MRG}, d_M, d_R, d_G, and $v_{s.QT}$. Formulas of the base indices (i.e. d_{BC}, d_{mr}, $v_{s.QL}$, $d_{BC'}$, d_{MRG}, and $v_{s.QT}$) are summarised in Table 1. All 11 indices were calculated for each survey interval for each plot. The latter six indices (i.e. $d_{BC'}$, d_{MRG}, d_M, d_R, d_G, and $v_{s.QT}$) were calculated for both basal area and bole biomass, distinguished by the suffixes '_area' or '_biomass', respectively. First, to show the contribution of each component to individual-based QT dissimilarity d_{MRG}, I estimated kernel density for each partitioned component (d_M, d_R, d_G, d_S, and d_E) of the dissimilarity indices. Second, I evaluated the relationships among d_{BC}, d_{mr}, $v_{s.QL}$, $d_{BC'}$, d_{MRG}, and $v_{s.QT}$ using simple linear regression. Third, to reveal the geographical and temporal components of the indices, I ran linear mixed models for each index. As explanatory variables, geographic factors (latitude and elevation), a temporal factor (mean calendar year between the first and second surveys), and a sampling design-related factor (length of survey interval) were used. Plot identity was considered a random effect in the model comparisons because 40 plots included two survey intervals. However, model comparisons showed that the linear mixed models consistently had higher Akaike information criterion (AIC; Akaike, 1998) values than the linear models (Table S1). Thus, all results discussed below are based on linear models.

All analyses were conducted using R software (ver. 4.1.0; R Development Core Team, 2021). The R packages *vegan* (Oksanen et al., 2020), *nlme* (Pinheiro et al., 2022), and *MuMIn* (Barton, 2022) were used to convert the abundance data to presence-absence data, run linear mixed models, and perform model comparisons based on AIC. The R scripts used to calculate the new indices are provided in Supplementary File 1.

For this case study, I did use not a dataset specifically constructed for climate change assessment; hence, it is not possible to directly test the hypothetical impacts of climate warming on compositional shifts in forest communities. However, it helps in understanding the mechanisms of the actual impact of climate change by considering

changes in individual factors. Although the present study focused on climate change, the indices introduced here can be useful in cases where individual growth rates vary over time for intrinsic reasons (e.g. ecological succession).

3. Results

Among the 126 survey intervals, the individual turnover of 10 survey intervals was zero; therefore, these intervals were excluded from the targets when calculating the $v_{s.QL}$ indices. The distribution of the novel indices, except $v_{s.QT}$, is shown in Fig. 3. The contribution of individual growth to the total turnover of both basal area and bole biomass was generally larger than those of mortality and recruitment (Fig. 3a, b; Fig. S3). The d_{MRG} indices based on basal area and bole biomass were strongly and positively correlated with d_{BC}, d_{mr}, area-based $d_{BC'}$, and biomass-based $d_{BC'}$ (≥0.87; Fig. S4). In contrast, the $v_{s.QT}$ indices based on basal area and bole biomass were only weakly correlated with the $d_{BC'}$ indices based on basal area and bole biomass (r = 0.23–0.28, Fig. S4) and showed no correlation with $v_{s.QL}$ (r = 0.16 and 0.08, Fig. S4). For both d_{MRG} and $v_{s.QT}$, strong correlations existed between the indices based on basal area and bole biomass (r = 0.99 and 0.91, Fig. S4). All Pearson correlation coefficients are summarised in Fig. S4.

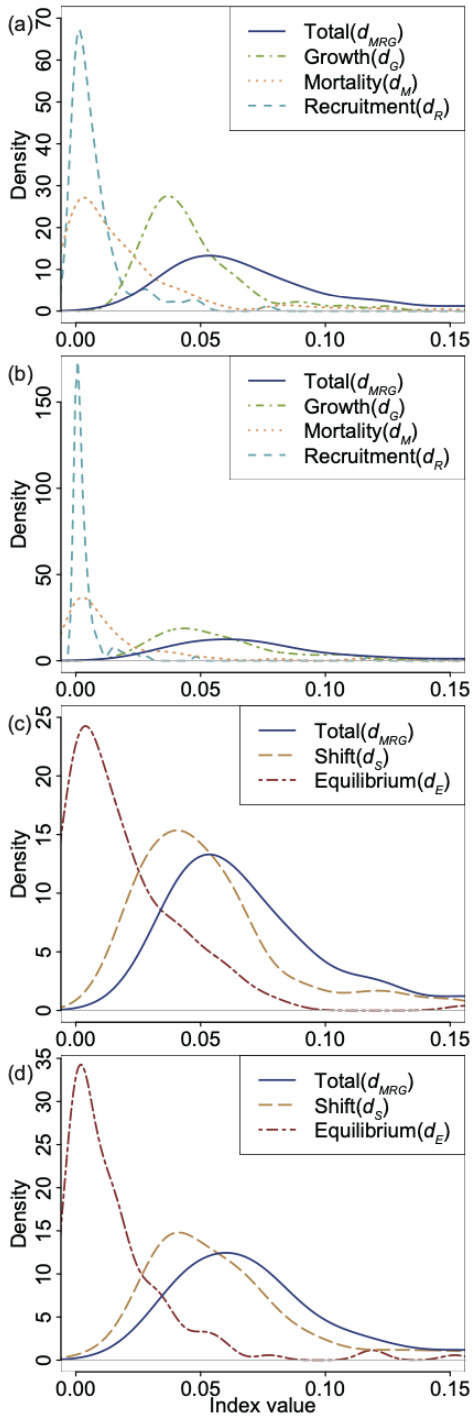

Fig. 3. Density plots representing the distribution of individual-based QT beta-diversity indices across 126 survey intervals for 86 plots (data from Stanke et al. 2020). In all four plots, the index values are limited to the range 0–0.15 to allow comparison (see Fig. S3 for a plot of the entire range). The plots in panels (a) and (c) are based on basal area, and those in (b) and (d) are based on bole biomass.

Based on AIC comparison, models including only intercept were selected for the three indices, i.e. the indices for compositional shift based on the number of individuals and basal area (d_{BC}, $d_{BC'_area}$) and the relative speed of compositional shift against total changes in basal area ($v_{s.QT_area}$) (Table 2). The index of compositional shift based on bole biomass ($d_{BC'_biomass}$) tended to increase with longer survey intervals as indicated by model comparison (Table 2). As for the index for the relative speed of compositional shift against total individual turnover ($v_{s.QL}$), only elevation was selected as an explanatory variable based on AIC comparison; thus, the index increased with increasing elevation (Table 2). For the relative speed of compositional shift against total changes in basal area ($v_{s.QT_biomass}$), a model including calendar year and survey interval was selected based on AIC comparison (Table 2); specifically, the index increased with increasing calendar year and longer survey intervals. In both indices of the total amount of change in basal area and bole biomass (d_{MRG_area}, $d_{MRG_biomass}$), models with latitude and survey interval were selected as the best models based on AIC comparisons (Table 2); specifically, the indices tended to increase with decreasing latitude and longer survey intervals. However, in the index of total individual turnover (d_{mr}), the model including only the survey interval was selected as the best model (Table 2), with the index increasing with longer survey intervals. As for the three indices related to the contribution of mortality to the total amount of change (d_m, d_{M_area}, $d_{M_biomass}$), models including latitude and calendar year were selected as the best models (Table 2), and index values tended to increase with decreasing latitude and increasing calendar year. For the indices related to the contribution of recruitment to the total amount of change (d_{R_area}, $d_{R_biomass}$), models including calendar year were selected as the best models (Table 2), with index values tending to increase with increasing calendar year. For the index related to the contribution of recruitment to the total individual turnover (d_r), the model including calendar year and survey interval was selected as the best model (Table 2), with the index tending to increase with increasing

calendar year and longer survey intervals. For both indices related to the contribution of growth to the total amount of change (d_{G_area}, $d_{G_biomass}$), the models that included the survey interval and, in the case of basal area, calendar year, were selected.

Table 2. Results of a multi-regression model based on the best models selected using an AIC comparison for individual-based qualitative (QL) and quantitative (QT) beta-diversity indices.

	Latitude				Elevation				Calendar year				Survey interval				*Adj R2*	*P-value*	
	β	*parR2*	*P-value*		β	*parR2*	*P-value*		β	*parR2*	*P-value*		β	*parR2*	*P-value*				
(a) Qualitative family indices																			
d_{BC}	–	–	–		–	–	–		–	–	–		–	–	–		†		
d_{mr}	–	–	–		–	–	–		–	–	–		0.0186	0.0089	0.1473		0.0089	0.1473	
d_m	-0.0807	0.0333	0.0233	*	–	–	–		0.0098	0.0953	0.0003	***	–	–	–		0.1211	0.0001	***
dr	–	–	–		–	–	–		-0.0129	0.0513	0.0064	**	0.0277	0.0146	0.0944	.	0.0554	0.0111	*
$v_{s.QL}$	–	–	–		0.0002	0.0283	0.0393	*	–	–	–		–	–	–		0.0283	0.0393	*
(b) Quantitative family indices																			
(i) Basal area																			
$d_{BC'}$	–	–	–		–	–	–		–	–	–		–	–	–		†		
d_{MRG}	-0.0705	0.0095	0.1413		–	–	–		–	–	–		0.0231	0.0192	0.0663	.	0.0269	0.0695	.
d_M	-0.0768	0.0253	0.0421	*	–	–	–		0.0094	0.0770	0.0010	**	–	–	–		0.0972	0.0007	***
d_R	–	–	–		–	–	–		-0.0044	0.0259	0.0398	*	–	–	–		0.0259	0.0398	*
d_G	–	–	–		–	–	–		-0.0028	0.0236	0.0477	*	0.0122	0.0381	0.0165	*	0.0305	0.0553	.
$v_{s.QT}$	–	–	–		–	–	–		–	–	–		–	–	–		†		
(ii) Bole biomass																			
$d_{BC'}$	–	–	–		–	–	–		–	–	–		0.0205	0.0114	0.1210		0.0114	0.1210	
d_{MRG}	-0.0748	0.0094	0.1429		–	–	–		–	–	–		0.0278	0.0264	0.0387	*	0.0336	0.0454	*
d_M	-0.0766	0.0209	0.0586	.	–	–	–		0.0092	0.0641	0.0026	***	–	–	–		0.0812	0.0020	**
d_R	–	–	–		–	–	–		-0.0039	0.0187	0.0684	.	–	–	–		0.0187	0.0685	.
d_G	–	–	–		–	–	–		–	–	–		0.0089	0.0227	0.0503	.	0.0227	0.0503	.
$v_{s.QT}$	–	–	–		–	–	–		-0.0301	0.0272	0.0366	*	0.0717	0.0082	0.1569		0.0232	0.0877	.

β and *parR2* indicate the regression coefficients and partially adjusted *R*-squared values of each explanatory variable, respectively. *Adj R2* is the adjusted *R*-squared value for the entire model. Note: Significance: .<0.1, *<0.05, **<0.01, ***<0.001. When a model with intercept only was selected, † is added into the column of *P*-value for the entire model.

4. Discussion

The potential for evaluating the contributions of individuals' persistence to compositional shifts in a community was first proposed by Nakadai (2020). Here, I extended the previously established individual-based beta-diversity approaches (Nakadai, 2020, 2021) to take account of individual property changes—even for persistent individuals—that are not currently considered in qualitative indices. Specifically, in addition to the components of mortality and recruitment as considered in Nakadai (2020), I for the first time introduced a growth component to account for the individual property changes in the context of compositional shifts (Fig. 1). Also, using hypothetical scenarios, I illustrated the biological meaning of the individual-based indices in the context of climate warming (Fig. 2). The novel indices proposed here not only represent methodological progress in community ecology and macroecology, but also provide a conceptual advance in bridging studies in biodiversity with those on individual life history and physiology.

To illustrate the application of the novel indices, I applied them to subset data from the FIA database for the state of Rhode Island (USA). The analysis demonstrated that the contribution of tree growth to the total turnover of both basal area and bole biomass was generally larger than those of mortality and recruitment (Fig. 3a, b; Fig. S3). This suggests the importance of previously overlooked growth factors in forest turnover and dynamics and the consequent compositional shifts. In the case-study dataset, the calculated abundance- and individual-based indices (i.e. d_{BC}, d_{mr}, $d_{BC'}$, and d_{MRG}) were strongly correlated (Fig. S4). Thus, if the contribution of individual tree growth is high, the strength of the correlation between d_{mr} and d_{MRG} should decrease, yet this was not the case. I found no clear relationships between the $v_{s.QL}$ and $v_{s.QT}$ indices based on both basal area and bole biomass and the relative speed of compositional shift. Generally, the values of $v_{s.QL}$ for the FIA dataset are high; thus, individual turnover generally contributed to compositional shift, although both $v_{s.QT_area}$ and $v_{s.QT_biomass}$ were lower and more variable than $v_{s.QL}$. These results reflect the differences in the characteristics of the novel QT indices developed here and the conventional QL indices. Indeed, $v_{s.QL}$ could not be applied to 10 plots that had no individual turnover, whereas in such cases, the $v_{s.QT}$ index was more sensitive to temporal changes in the community than the $v_{s.QL}$ index.

In the driver analysis of the calculated indices, I found that various explanatory variables affected the results (Table 2). First, focusing on the growth component specific to the new QT index, both area- and biomass-based d_G indices, which indicate the contribution of growth, were responsive to the survey interval. This strongly suggests that an accurate evaluation of the contribution of growth was achieved. In addition, the area-based d_G index tended to decrease with increasing (i.e. more recent) calendar year. In addition, overall, the contributions related to recruitment decreased, and those related to mortality increased (Table 2), which may be indicative of succession (i.e. aging forests) and/or climate change.

The $v_{s.QT_area}$ index showed no clear pattern because the model including intercept only was selected, whereas the $v_{s.QL}$ and $v_{s.QT_biomass}$ indices varied with elevation and calendar year, respectively. The v_s family of indices is designed to capture changes to account for stochastic drifts, such as individual, basal-area, or bole-volume turnover. The significant relationships between several v_s indices with environmental variables suggest that along with the explanatory variables, niche processes drive compositional shifts, which cannot be explained by stochastic processes alone. For example, Nakadai (2020) showed that $v_{s.QL}$ values vary along climate gradients (i.e. the change ratio of annual mean temperature) for both deciduous and evergreen broadleaf forests.

Although the indices I have introduced here are mainly applicable to datasets containing both individual identity and property information, a method that accommodates various types of quantitative individual information may become available through future theoretical developments. Generally, information for individuals is limited in community ecology and macroecology, yet in the era of big data, this is likely to be addressed in the near future. In addition, if the contributions of demographic factors (i.e. growth, mortality, and recruitment) can be estimated using hierarchical modelling approaches (e.g. Hill et al., 2004, Kanamori et al., 2017), these indices could be calculated even in the absence of detailed individual-tracking information.

Notably, climate change affects various ecological hierarchies, from global biodiversity to individuals and even intra-individual phenomena (Arneth et al., 2020; Körner, 2017). Applying the individual-based beta-diversity indices to global datasets, especially forest inventory data (e.g. ForestGEO; https://forestgeo.si.edu/), is, therefore, highly promising for assessing the impacts of global climate change. Indeed, individual-based diversity indices

able to account for previously overlooked elements of biodiversity, such as individual persistence and growth, open the door to innovative individual-based biodiversity research. This should facilitate a greater understanding of the effects of climate change across multiple hierarchies of biological organisation.

Author contributions

Ryosuke Nakadai: Conceptualization, Methodology, Formal analysis, Writing – original draft, review & editing.

Funding

RN was supported by the Japan Society for the Promotion of Science (grant No. 22K15188) and the National Institute for Environmental Studies, Japan.

Conflicts of interest

The author declares no conflicts of interest.

Data availability

Data are available from the package rFIA (Stanke et al., 2020) in R, and the code used to calculate the indices in the present study is provided in Supplementary File 1.

References

Akaike, H. (1998). Information theory and an extension of the maximum likelihood principle. In: E. Parzen, K. Tanabe, and G. Kitagawa (Eds.), Selected Papers of Hirotugu Akaike. Springer, New York, pp. 199–213. doi:10.1007/978-1-4612-1694-0_15

Arneth, A., Shin, Y. J., Leadley, P., Rondinini, C., Bukvareva, E., Kolb, M., . . . Saito, O. (2020). Post-2020 biodiversity targets need to embrace climate change. Proc. Natl. Acad. Sci. U. S. A. 117, 30882–30891. doi:10.1073/pnas.2009584117

Bartoń, K. (2020). MuMIn: Multi-model inference. R package version 1.43.17. https://CRAN.R-project.org/package=MuMIn.

Baselga, A. (2013). Separating the two components of abundance-based dissimilarity:

balanced changes in abundance vs. abundance gradients. Methods Ecol. Evol. 4, 552–557. doi:10.1111/2041-210X.12029

Brienen, R. J. W., Caldwell, L., Duchesne, L., Voelker, S., Barichivich, J., Baliva, M., Ceccanthini, G., Di Fillippo, A., Helama, S., Locosselli, G. M., Lopez, L. Piovesan, J., Villabla, R., Gloor, E. (2020). Forest carbon sink neutralized by pervasive growth-lifespan trade-offs. Nat. Commun. 11, 4241. https://doi.org/10.1038/s41467-020-17966-z

Brienen, R., Phillips, O., Feldpausch, T. Gloor, E., Baker, T., Lloyd, J., Lopez-Gonzalez, G., Monteagudo-Mendoza, A., Malhi, Y., Lewis, S. L., Vásquez Martinez, R., Alexiades, M., Álvarez Dávila, E., Alvarez-Loayza, P., Andrade, A., Aragão, L. E. O. C., Araujo-Murakami, A., Arets, E. J. M. M., Arroyo, L., Aymard C. G. A., Bánki, O. S., Baraloto, C., Barroso, J., Bonal, D., Boot, R. G. A., Camargo, J. L. C., Castilho, C. V., Chama, V., Chao, K. J., Chave, J., Comiskey, J. A., Cornejo Valverde, F., da Costa, L., de Oliveira, E. A., Di Fiore, A., Erwin, T. L., Fauset, S., Forsthofer, M., Galbraith, D. R., Grahame, E. S., Groot, N., Hérault, B., Higuchi, N., Honorio Coronado, E. N., Keeling, H., Killeen, T. J., Laurance, W. F., Laurance, S., Licona, J., Magnussen, W. E., Marimon, B. S., Marimon-Junior, B. H., Mendoza, C., Neill, D. A., Nogueira, E. M., Núñez, P., Pallqui Camacho, N. C., Parada, A., Pardo-Molina, G., Peacock, J., Peña-Claros, M., Pickavance, G. C., Pitman, N. C. A., Poorter, L., Prieto, A., Quesada, C. A., Ramírez, F., Ramírez-Angulo, H., Restrepo, Z., Roopsind, A., Rudas, A., Salomão, R. P., Schwarz, M., Silva, N., Silva-Espejo, J. E., Silveira, M., Stropp, J., Talbot, J., ter Steege, H., Teran-Aguilar, J., Terborgh, J., Thomas-Caesar, R., Toledo, M., Torello-Raventos, M., Umetsu, R. K., van der Heijden, G. M. F., van der Hout, P., Guimarães Vieira, I. C., Vieira, S. A., Vilanova, E., Vos, V. A., Zagt, R. J. (2015). Long-term decline of the Amazon carbon sink. Nature 519, 344–348. https://doi.org/10.1038/nature14283

Brown, J. H., Gillooly, J. F., Allen, A. P., Savage, V. M., West, G. B. (2004). Toward a metabolic theory of ecology. Ecology 85, 1771–1789. doi:10.1890/03-9000

Brown, J. H. (1995). Macroecology. University of Chicago Press.

Brown, J. H. (1999). Macroecology: Progress and prospect. Oikos 87, 3–14. doi:10.2307/3546991

Burrill, E. A., DiTommaso A. M., Turner, J. A., Pugh, S. A., Menlove, J., Christiansen, G., Perry, C. J., Conkling, B. L. (2021). The forest inventory and analysis database: Database description and user guide version 9.0.1 for Phase 2. U.S. Department of Agriculture, Forest Service, p. 1026. http://www.fia.fs.fed.us/library/database-

documentation/

Domke, G. M., Oswalt, C. M., Woodall, C. W., Turner, J. A. (2013). Estimation of merchantable bole volume and biomass above sawlog top in the National Forest Inventory of the United States. J. For. 111, 383–387. doi:10.5849/jof.13-042

Dornelas, M., Gotelli, N. J., Mcgill, B., Shimadzu, H., Moyes, F., Sievers, C., Magurran, A. E. (2014). Assemblage time series reveal biodiversity change but not systematic loss. Science 344, 296–299. doi:10.1126/science.1248484

García Molinos, J., Halpern, B. S., Schoeman, D. S., Brown, C. J., Kiessling, W., Moore, P. J., Pandolfi, J. M., Poloczanska, E. S., Richardson, A. J., Burrows, M. T. (2016). Climate velocity and the future global redistribution of marine biodiversity. Nat. Clim. Change 6, 83–88. doi:10.1038/nclimate2769

Gotelli, N. J., Shimadzu, H., Dornelas, M., McGill. B., Moyes. F., Magurran, A. E. (2017). Community-level regulation of temporal trends in biodiversity. Sci. Adv. 3, e1700315. doi:10.1126/sciadv.1700315

Hill, M. F., Witman, J. D., Caswell, H. (2004). Markov chain analysis of succession in a rocky subtidal community. Am. Nat. 164, 46–61. doi:10.1086/422340

Kanamori Y., Fukaya, K., Noda, T. (2017). Seasonal changes in community structure along a vertical gradient: Patterns and processes in rocky intertidal sessile assemblages. Popul. Ecol. 59, 301–313. doi:10.1007/s10144-017-0596-z

Körner, C. (2017). A matter of tree longevity. Science 355, 130–131. doi:10.1126/science.aal2449

Legendre, P., Legendre, L. (2012). Numerical ecology (3rd ed.). Amsterdam: Elsevier.

Legendre, P. (2019). A temporal beta-diversity index to identify sites that have changed in exceptional ways in space–time surveys. Ecol. Evol. 9, 3500–3514. doi:10.1002/ece3.4984

Li, S. P., Cadotte, M. W., Meiners, S. J., Pu, Z., Fukami, T., Jiang, L. (2016). Convergence and divergence in a long-term old-field succession: The importance of spatial scale and species abundance. Ecol. Lett. 19, 1101–1109. doi:10.1111/ele.12647

Magurran, A. E. (2011). Measuring biological diversity in time (and space). In A. Magurran & B. J. McGill (Eds.), Biological diversity: Frontiers in measurement and assessment. Oxford University Press, Oxford, pp. 85–104.

Magurran, A. E., Dornelas, M., Moyes, F., Henderson, P. A. (2019). Temporal β diversity: A macroecological perspective. Glob. Ecol. Biogeogr. 28, 1949–1960. doi:10.1111/geb.13026

Magurran, A. E., Dornelas, M., Moyes, F., Gotelli, N. J., McGill, B. (2015). Rapid biotic homogenization of marine fish assemblages. Nat. Commun. 6, 8405. doi:10.1038/ncomms9405

Munné-Bosch, S. (2018). Limits to tree growth and longevity. Trends Plant Sci. 23, 985–993. doi:10.1016/j.tplants.2018.08.001

Nakadai, R. (2020). Degrees of compositional shift in tree communities vary along a gradient of temperature change rates over one decade: Application of an individual-based temporal beta-diversity concept. Ecol. Evol. 10, 13613–13623. doi:10.1002/ece3.6579

Nakadai, R. (2021). Individual-based multiple-unit dissimilarity: novel indices and null model for assessing temporal variability in community composition. Oecologia 197, 353–364. doi:10.1007/s00442-021-05025-3

Odum, E. P. (1950). Bird populations of the Highlands (North Carolina) Plateau in relation to plant succession and avian invasion. Ecology 31, 587–605. doi:10.2307/1931577

Oksanen, J., Blanchet, F. G., Friendly, M., Kindt, R., Legendre, P., McGlinn, D., Minchin, P. R., O'Hara, R. B., Simpson, G. L., Solymos, P., Stevens, M. H. H., Scöcs, E., Wagner, H. H. (2020). Vegan: Community ecology package. R package version 2.5-7. https://CRAN.R-project.org/package=vegan

Pinheiro, J., Bates, D., DebRoy, S., Sarkar, D., R Core Team. (2022). Nlme: Linear and nonlinear mixed effects models. R package version 3.1-155. https://CRAN.R-project.org/package=nlme

R Development Core Team. (2021). R: A language and environment for statistical computing. R Foundation for Statistical Computing, Vienna, Austria. (ver. 4.1.0). http://www.R-project.org/

Searle, E. B., Chen, H. Y. (2018). Temporal declines in tree longevity associated with faster lifetime growth rates in boreal forests. Environ. Res. Lett. 13, 125003. doi:10.1088/1748-9326/aaea9e

Shimadzu, H. Dornelas, M., Magurran, A. E. (2015). Measuring temporal turnover in ecological communities. Methods Ecol. Evol. 6, 1384–1394. doi:10.1111/2041-

210X.12438

Sørensen, T. A. (1948). A method of establishing groups of equal amplitude in plant sociology based on similarity of species content and its application to analyses of the vegetation on Danish commons. Biol. Skr. 5, 1–34.

Stanke, H., Finley, A. O., Weed, A. S., Walters, B. F., Domke, G. M. (2020). rFIA: An R package for estimation of forest attributes with the US Forest Inventory and Analysis database. Environ. Model. Softw. 127, 104664. doi:10.1016/j.envsoft.2020.104664

Tatsumi, S., Iritani, R., Cadotte, M. W. (2021). Temporal changes in spatial variation: Partitioning the extinction and colonisation components of beta diversity. Ecol. Lett. 24, 1063–1072. doi:10.1111/ele.13720

Vellend, M., Baeten, L., Myers-Smith I. H., Elmendorf, S. C., Beauséjour, R., Brown C. D., De Frenne, P., Verheyen, K., Wipf, S. (2013). Global meta-analysis reveals no net change in local-scale plant biodiversity over time. Proc. Natl. Acad. Sci. U. S. A. 110, 19456–19459. doi:10.1073/pnas.1312779110

Supplementary files

Table S1. Comparison of linear and linear mixed models for each index. The best models selected from the comparison are shown in Table 2

Fig. S1. Venn diagrams related to the calculation of both conventional and novel indices. Specifically, the first four Venn diagrams (a–d) are based on the number of individuals, and latter four (e–h) are based on the total amount of targeted measures excluding the number of individuals (e.g. sizes and weights).

Fig. S2. Map of geographic locations of plots included in the subset dataset from the Forest Inventory and Analysis (FIA) database for the state of Rhode Island (USA) (Stanke et al., 2020). Sites indicated with darker coloured points have multiple survey intervals.

Fig. S3. Density plots representing the distribution of individual-based quantitative beta-diversity indices across 126 survey intervals in 86 plots (data from Stanke et al., 2020). In the right four plots (b, d, f, and h), the index values are limited to the range 0–0.15 to allow comparison (also see Fig. 2). In the left four plots, the entire value range is shown. Plots in panels (a), (b), (e), and (f) are based on the basal area, and those in panels (c), (d), (g), and (h) on bole biomass.

Fig. S4. Correlations among the calculated indices. Pearson coefficients of correlation are shown. Note: Significance: .<0.1, *<0.05, **<0.01, ***<0.001.

Supplementary text 1. Explanation of individual-based temporal beta diversity employing the Ružička dissimilarity index.

Supplementary file 1. R software script for individual-based temporal beta-diversity calculations using sample data.